PHYSICAL REVIEW B **79**, 060509(R) (2009)

Geometrical dependence of the low-frequency noise in superconducting flux qubits

T. Lanting,[1,*] A. J. Berkley,[1] B. Bumble,[2] P. Bunyk,[1] A. Fung,[2] J. Johansson,[1] A. Kaul,[2] A. Kleinsasser,[1] E. Ladizinsky,[1] F. Maibaum,[1] R. Harris,[1] M. W. Johnson,[1] E. Tolkacheva,[1] and M. H. S. Amin[1]

[1]*D-Wave Systems Inc., 100-4401 Still Creek Drive, Burnaby, British Columbia, Canada V5C 6G9*

[2]*Jet Propulsion Laboratory, California Institute of Technology, Pasadena, California 91109, USA*

(Received 1 December 2008; published 26 February 2009)

A general method for directly measuring the low-frequency flux noise (below 10 Hz) in compound Josephson-junction superconducting flux qubits has been used to study a series of 85 devices of varying design. The variation in flux noise across sets of qubits with identical designs was observed to be small. However, the levels of flux noise systematically varied between qubit designs with strong dependence upon qubit wiring length and wiring width. Furthermore, qubits fabricated above a superconducting ground plane yielded lower noise than qubits without such a layer. These results support the hypothesis that local impurities in the vicinity of the qubit wiring are a key source of low-frequency flux noise in superconducting devices.

DOI: 10.1103/PhysRevB.79.060509 PACS number(s): 74.40.+k, 85.25.Am

Qubits implemented in superconducting integrated circuits show considerable promise as building blocks of scalable quantum processors. However, low-frequency noise in superconducting devices places fundamental limitations on their use in quantum information processing.[1–4] Recent theoretical work has highlighted several potential sources for low-frequency noise. These include ensembles of two-level systems (TLSs) that could be associated with dielectric defects,[5–7] magnetic impurities in surface oxides on superconducting wiring,[8] and flux noise induced by spin flips at dielectric interfaces.[9] Characterizing low-frequency noise is an essential step in understanding its mechanism and in developing fabrication strategies to minimize its amplitude. Several techniques have been exploited to indirectly measure low-frequency noise in superconducting qubits.[10,11] This Rapid Communication describes a technique for directly measuring low-frequency noise in rf superconducting quantum interference device (SQUID) flux qubits. We present measurements performed on a series of qubits of varying wiring lengths and widths, and qubits with and without superconducting shielding layers.

The devices described in this Rapid Communication were fabricated on an oxidized Si wafer with a $Nb/Al/Al_2O_3/Nb$ trilayer process. There were two additional wiring layers, WIRA and WIRB, above the trilayer [see Fig. 1(a)]. All wiring layers were insulated from each other with layers of sputtered SiO_2. 85 qubits with a range of geometries (wiring length, wiring width, and the presence or absence of shielding planes) were tested. Qubit wiring lengths ranged from 350 μm to 2.1 mm and wiring widths ranged from 1.4 to 3.5 μm. Moreover, the qubits were drawn from several wafers to control for variability in fabrication process conditions.

The compound Josephson-junction (CJJ) rf SQUID is shown schematically in Fig. 1(b) and consists of a small CJJ loop (inductance $\sim$10 pH) and the main qubit loop (inductances vary from $\sim$80 to $\sim$800 pH). The loops are externally flux biased with Φ_x^{CJJ} and Φ_x^q, respectively. The CJJ loop contains two Josephson junctions with critical current I_c^q when connected in parallel. For $L_{\mathrm{CJJ}} \ll L_q$ the Hamiltonian for an isolated device can be approximately expressed as[12]

$$H_{\mathrm{rf}}(\Phi^q, Q) = \frac{1}{2C^q} Q^2 + U(\Phi^q), \tag{1}$$

$$U(\Phi^q) = \frac{(\Phi^q - \Phi_x^q)^2}{2L^q} - E_J \cos\left[\frac{\pi \Phi_x^{\mathrm{CJJ}}}{\Phi_0}\right] \cos\left[\frac{2\pi \Phi^q}{\Phi_0}\right], \tag{2}$$

where Φ^q is the total flux, Q is the charge stored in the net capacitance C^q across the junctions, $E_J = \Phi_0 I_c^q / 2\pi$, and $\Phi_0 = h/2e$. The potential energy $U(\Phi_q)$ is monostable when $\beta = 2\pi L_q I_c \cos(\pi \Phi_x^{\mathrm{CJJ}} / \Phi_0) / \Phi_0 < 1$ and classically bistable with two countercirculating persistent current states (denoted as $|0\rangle$ and $|1\rangle$) possessing persistent current of magnitude $|I_p| = |\langle n | \Phi^q / L^q | n \rangle|$ for $\beta > 1$. Ignoring all but the two lowest-energy levels (two-level approximation), one can map an isolated CJJ rf SQUID onto a qubit Hamiltonian,

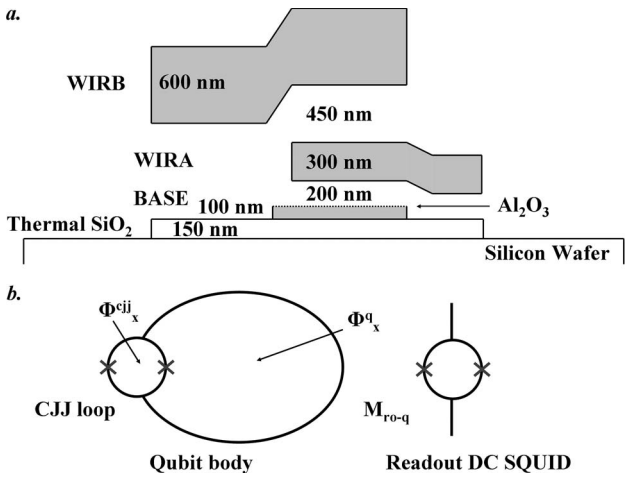

FIG. 1. (a) Cross section of the fabrication stack. There are three Nb metal layers: BASE, WIRA, and WIRB. The trilayer is grown on the top of the BASE layer. Wiring layers are insulated from each other with layers of sputtered SiO_2. (b) CJJ rf-SQUID qubit schematic.

$$H_q = -\frac{1}{2}[\epsilon\sigma_z + \Delta\sigma_x], \tag{3}$$

where $\epsilon = 2|I_p|\Phi_x^q$ is the energy bias, Δ is the tunneling energy between $|0\rangle$ and $|1\rangle$, and σ_z and σ_x are Pauli matrices. For an rf-SQUID qubit both $|I_p|$ and Δ are functions of Φ_x^{CJJ}. A dc SQUID, inductively coupled to the qubit with mutual inductance $M_{\text{ro-}q}$, distinguishes between the qubit states by measuring the flux generated by the persistent current for $\Phi_x^{\mathrm{CJJ}} = n\Phi_0$ where $\Delta \approx 0$.

Our qubit magnetometry technique consists of initializing the qubit at its degeneracy point $(\Phi_x^{\mathrm{CJJ}} = \Phi_0/2, \Phi^q = 0)$, raising the tunnel barrier by applying a 30 μs linear ramp from $\Phi_x^{\mathrm{CJJ}} = \Phi_0/2$ to $\Phi_x^{\mathrm{CJJ}} = \Phi_0$ to localize the qubit in $|0\rangle$ or $|1\rangle$ and then measuring its state with the dc SQUID. We repeat this bias and measure cycle n times, assigning each $|0\rangle$ measurement a value 0 and each $|1\rangle$ measurement a value 1. We then average these n measurements to produce a population measurement $P \in [0,1]$ which has an uncertainty $1/\sqrt{4n}$. In the absence of flux noise one would expect $P = 0.5$. However, in the presence of low-frequency flux noise, the population measurements will fluctuate about $P = 0.5$ with an amplitude that depends on the noise scale. We can thus use P to directly probe the flux environment experienced by the qubit as a function of time.

To calibrate the mapping from P to flux noise amplitude we first measured the flux periodicity of the rf SQUID. We then assume a phenomenological form for population versus external flux bias

$$P(\Phi_x^q, t) = \frac{1}{2}\left[1 + \tanh\left(\frac{\Phi_x^q + \Phi_n(t) - \Phi_0^q}{2\delta}\right)\right], \tag{4}$$

where $\Phi_n(t)$ is a time-dependent flux noise, Φ_0^q is the external flux needed to balance $P = 0.5$ $(\epsilon = 0)$, and δ captures the breadth of the transition. With sufficient averaging, we measure a static population distribution $\overline{P(\Phi_x^q)} = \frac{1}{2}[1 + \tanh(\frac{\Phi_x^q - \Phi_0^q}{2\delta})]$ which allows us to calibrate Φ_0^q and δ [see Fig. 2(a)]. Inverting Eq. (4) then allows one to convert measurements of P to $\Phi_n(t)$.

Figure 2 shows example qubit magnetometry measurements. Each flux measurement is derived from 128 population measurements. Time traces were collected for 325 s. The white-noise level of the resulting power spectral density (PSD) is consistent with the error expected from a binomial distribution of population measurements. At a fixed temperature this noise level can be reduced by sampling at a higher frequency. In practice, we are limited to a sample frequency of 5 kHz by the bandwidth of the control lines connecting the qubit to the room-temperature electronics.

In addition to the aforementioned white noise, a typical PSD also shows a $1/f$ frequency dependence for $f < 10$ Hz. To separate the contribution to the PSD from white noise and $1/f$ noise, we define the $1/f$ contribution as

$$S_\Phi(f) = A\left(\frac{1\ \mathrm{Hz}}{f}\right)^{+\alpha} \tag{5}$$

and fit the measured PSD from every qubit tested with the function

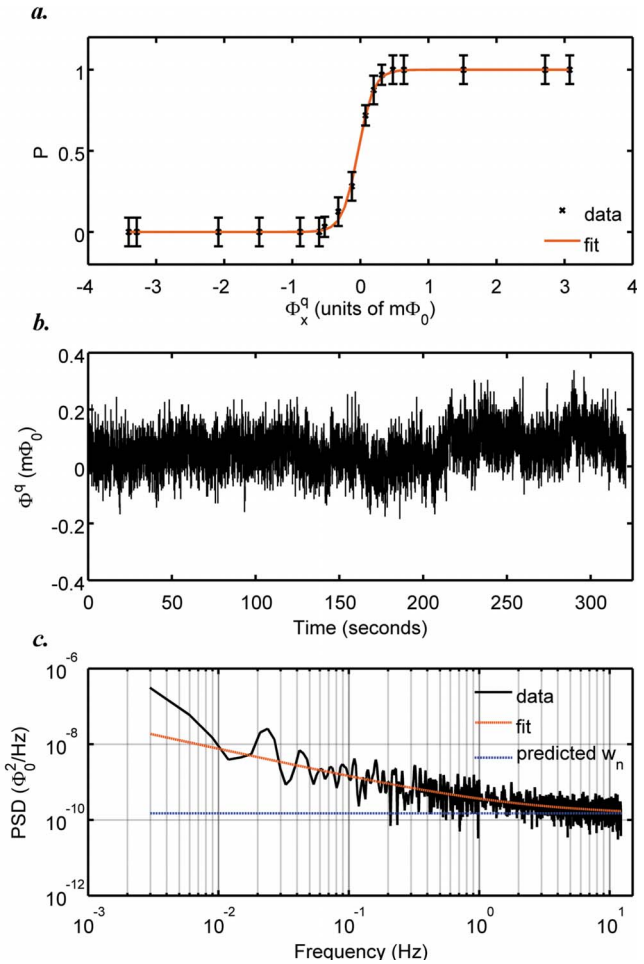

FIG. 2. (Color online) Flux noise measurements for a typical qubit. (a) Static qubit population P vs external flux bias. The fit is shown in red (gray). (b) Qubit flux versus time. (c) Power spectral density of flux signal. The fit to Eq. (6) is shown in red (gray) and the white-noise level expected from a binomial distribution is shown in blue (dashed).

$$\mathrm{PSD}(f) = S_\Phi(f) + w_n, \tag{6}$$

where A represents the magnitude of the $1/f$ noise at 1 Hz (Φ_0^2/Hz), α represents the power of the frequency dependence, and w_n represents the white-noise level. We interpret the $1/f$ power extracted from the PSD fit as a low-frequency flux noise signal $S_\Phi(f)$ that biases the qubit.[13] Measurements of the current noise of the room-temperature current sources that provide Φ_x^q reveal that their low-frequency noise is over a factor of 50 below the smallest measured S_Φ. The fit values of α were clustered around $\alpha = 1.00 \pm 0.15$.

To investigate the variation in the low-frequency noise between qubits of identical design, we measured a set of 27 identical qubits (700 μm long and 1.4 μm wide). Figure 3 shows a histogram of the low-frequency flux noise $S_\Phi(1\ \mathrm{Hz})$ for these qubits. We measure a median $A = 1.9 \pm 0.3 \times 10^{-10}\Phi_0^2/\mathrm{Hz}$.

In Fig. 4(a) we compare the value of A as a function of wiring length for qubits that are 1.4 μm wide and have a shielding plane under the qubit wiring. A fit of the form

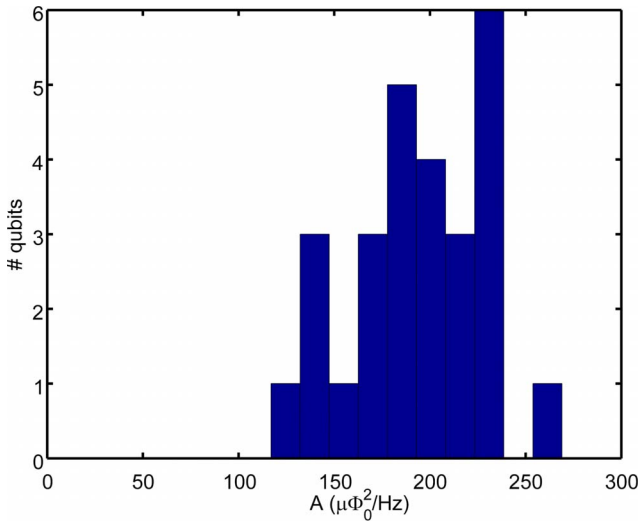

FIG. 3. (Color online) Variation in qubit flux noise across 27 identical qubits.

$S_\Phi(1\ \mathrm{Hz})=A_0L^\beta$ yielded $A_0=1.7\pm0.3\times10^{-10}\Phi_0^2/\mathrm{Hz}$ and $\beta=1.14\pm0.15$. A_0 measures the $1/f$ power scaled to a length of 350 μm and β measures the scaling with length. The $1/f$ power scales approximately linearly with the wiring length of the qubit. Performing the same comparison for qubits that are 3.5 μm wide and have no shielding plane yields $A_0=9.5\pm0.3\times10^{-11}\Phi_0^2/\mathrm{Hz}$ and $\beta=1.1\pm0.25$.

In Fig. 4(b) we compare the $1/f$ noise as a function of wiring width in qubits that are 350 μm long and have no shielding plane. We see a dependence on the $1/f$ amplitude with qubit width. A fit of the results to the form $S_\Phi(1\ \mathrm{Hz})=B_0w^\gamma$, where B_0 measures the $1/f$ power scaled to a width of 1 μm and γ measures the scaling with width. The fit yielded $B_0=9.6\pm0.5\times10^{-10}\Phi_0^2/\mathrm{Hz}$ and $\gamma=-0.98\pm0.10$. The $1/f$ power scales approximately as the inverse of the wiring width of the qubit.

There are clear differences in qubits that are geometrically identical except for the presence or absence of a ground plane underneath the device. Table I shows a comparison of the measured noise between such pairs of qubits. In all cases, qubits with a ground plane underneath the device were quieter by 30%–50%.

TABLE I. Comparison of qubits with and without BASE shielding.

Description	Shield	$\sqrt{S_\Phi(1\ \mathrm{Hz})}(\mu\Phi_0/\sqrt{\mathrm{Hz}})$
WIRA, $L=2.1$ mm, $w=3.5$ μm	Yes	17 ± 1
WIRA, $L=2.1$ mm, $w=3.5$ μm	No	25 ± 4
WIRB, $L=2.1$ mm, $w=1.4$ μm	Yes	29 ± 2
WIRB, $L=2.1$ mm, $w=1.4$ μm	No	34 ± 4
WIRA, $L=1.4$ mm, $w=3.5$ μm	Yes	15 ± 2
WIRA, $L=1.4$ mm, $w=3.5$ μm	No	21 ± 2
WIRA, $L=1.4$ mm, $w=1.4$ μm	Yes	21 ± 2
WIRA, $L=1.4$ mm, $w=1.4$ μm	No	27 ± 2
WIRB, $L=1.4$ mm, $w=1.5$ μm	Yes	21 ± 2
WIRB, $L=1.4$ mm, $w=1.5$ μm	No	27 ± 3

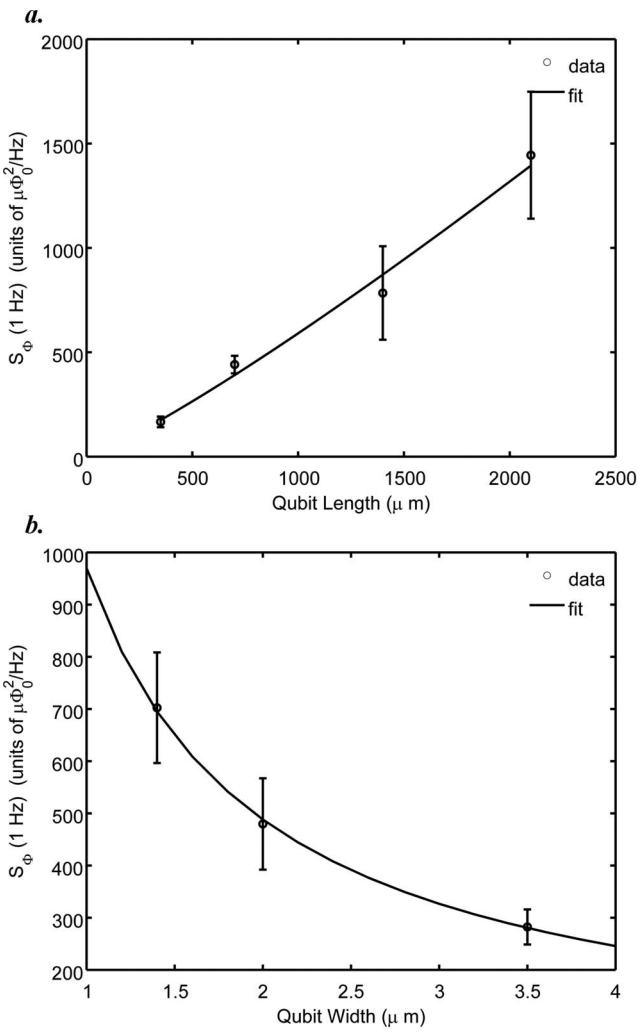

FIG. 4. (a) Qubit noise for different wiring lengths and a shielding plane under the qubit. (b) Qubit noise for different wiring widths, no ground plane is present.

Qubit magnetometry on this series of devices has revealed a clear dependence of the low-frequency noise on geometry. The scaling with wiring length and width suggests a noise source local to the qubit wiring. For example, the microscopic model described in Refs. 8 and 14 suggests low-frequency noise due to localized but interacting magnetic moments (the most likely candidate is defects in Nb_2O_5 layers on the qubit wiring) where the power should scale as L/w for a qubit of length L and width w. While this model predicts a noise amplitude and geometrical dependence in rough agreement with the results reported herein, the model also predicts a high-frequency cutoff of $f_c\sim100$ Hz with white noise at frequencies below f_c. Our data show a clear frequency dependence down to 10^{-2} Hz which disagrees with this prediction.

The measurements also reveal that qubits with a shielding plane under their wiring are systematically quieter than qubits with shielding over their wiring or qubits with no shielding plane (Table II). For qubits with underlying shielding layers, current flow is predominantly distributed along the bottom surface of the qubit wiring. This surface is naturally

TABLE II. Comparison of qubits with shielding above and below the qubit wiring.

Description	Shield	$\sqrt{S_\Phi(1\ \mathrm{Hz})}(\mu\Phi_0/\sqrt{\mathrm{Hz}})$
WIRA, $L=0.7$ mm, $w=1.4$ μm	Under	18 ± 1
WIRA, $L=0.7$ mm, $w=1.4$ μm	Over	21 ± 1
WIRA, $L=2.1$ mm, $w=1.4$ μm	Under	26 ± 2
WIRA, $L=2.1$ mm, $w=1.4$ μm	Over	38 ± 2
WIRA, $L=1.4$ mm, $w=1.4$ μm	Under	21 ± 2
WIRA, $L=1.4$ mm, $w=1.4$ μm	Over	28 ± 2

protected from subsequent fabrication and ambient conditions and should exhibit fewer impurities. Note also that shielding under the qubit wiring isolates the qubit from the Si/SiO_2 interface on the substrate. Impurities at this interface could be responsible for coupling flux into the qubit, and some models predict a frequency-dependent noise.[9]

The magnetometry technique described in this Rapid Communication is an effective way of probing low-frequency flux noise in superconducting flux qubits. This technique revealed that qubits having varying lengths, widths, and shielding are subject to systematically different levels of noise. The behavior of the measured flux noise is in approximate agreement with theoretical microscopic models that postulate that the source of flux noise is the magnetic impurities proximal to the qubit wiring. However, the measurements do not rule out local impurities in the dielectric insulating layers. These measurements suggest that to reduce low-frequency noise in superconducting qubits, the ratio of qubit length to width should be reduced as much as possible. A shielding layer close to the qubits and preferably between the qubit wiring and the Si/SiO_2 interface further reduces flux noise.

We thank D. Averin, J. Hilton, G. Rose, G. Dantsker, C. Rich, E. Chapple, P. Spear, F. Cioata, B. Wilson, and F. Brito for useful discussions. Samples were fabricated by the Microelectronics Laboratory of the Jet Propulsion Laboratory, operated by the California Institute of Technology under a contract with NASA.

*tlanting@dwavesys.com

[1] R. Koch, J. Clarke, J. Martinis, W. Goubau, C. Pegrum, and D. Harlingen, IEEE Trans. Magn. **19**, 449 (1983).

[2] F. Yoshihara, K. Harrabi, A. O. Niskanen, Y. Nakamura, and J. S. Tsai, Phys. Rev. Lett. **97**, 167001 (2006).

[3] F. C. Wellstood, C. Urbina, and J. Clarke, Appl. Phys. Lett. **50**, 772 (1987).

[4] F. Wellstood, C. Urbina, and J. Clarke, IEEE Trans. Magn. **23**, 1662 (1987).

[5] R. W. Simmonds, K. M. Lang, D. A. Hite, S. Nam, D. P. Pappas, and J. M. Martinis, Phys. Rev. Lett. **93**, 077003 (2004).

[6] J. M. Martinis *et al.*, Phys. Rev. Lett. **95**, 210503 (2005).

[7] R. H. Koch, D. P. DiVincenzo, and J. Clarke, Phys. Rev. Lett. **98**, 267003 (2007).

[8] L. Faoro and L. B. Ioffe, Phys. Rev. Lett. **100**, 227005 (2008).

[9] R. de Sousa, Phys. Rev. B **76**, 245306 (2007).

[10] R. Harris *et al.*, Phys. Rev. Lett. **98**, 177001 (2007).

[11] R. C. Bialczak *et al.*, Phys. Rev. Lett. **99**, 187006 (2007).

[12] R. Harris *et al.*, Phys. Rev. Lett. **101**, 117003 (2008).

[13] Another potential source of noise in our devices is the fluctuations in the junctions themselves. We have independently estimated the level of low-frequency critical current noise in the qubit junctions. We can place an upper limit of $\sqrt{S_{I_c}(1\ \mathrm{Hz})}=3\times10^{-6}$ at 1 Hz on relative I_c fluctuations in our junctions. The flux noise we are measuring is too large to be explained by the I_c fluctuations.

[14] S. Sendelbach, D. Hover, A. Kittel, M. Mück, J. M. Martinis, and R. McDermott, Phys. Rev. Lett. **100**, 227006 (2008).